www.impactjournals.com/oncotarget/ Oncotarget, 2017, Vol. 8, (No. 66), pp: 110289-110299

Research Paper

Accelerated atherogenesis in completely ligated common carotid artery of apolipoprotein E-deficient mice

Zhihui Chang[1,2], Chaoji Huangfu[1,3], Andrew T. Grainger[4], Jingang Zhang[3], Qiyong Guo[2] and Weibin Shi[1,4]

[1]Department of Radiology & Medical Imaging, University of Virginia, Charlottesville, Virginia, USA

[2]Department of Radiology, Shengjing Hospital of China Medical University, Shenyang, China

[3]Beijing Key Laboratory of Blood Safety and Supply Technologies, Beijing Institute of Transfusion Medicine, Beijing, China

[4]Biochemistry & Molecular Genetics, University of Virginia, Charlottesville, Virginia, USA

Correspondence to: *Weibin Shi,* ***email:*** *ws4v@virginia.edu*

Keywords: *atherosclerosis; hyperlipidemia; neovessel; foam cell; mice*

Received: *August 31, 2017* ***Accepted:*** *November 05, 2017* ***Published:*** *November 25, 2017*

Copyright: Chang et al. This is an open-access article distributed under the terms of the Creative Commons Attribution License 3.0 (CC BY 3.0), which permits unrestricted use, distribution, and reproduction in any medium, provided the original author and source are credited.

ABSTRACT

Complete ligation of the common carotid artery near its bifurcation induces neointimal formation due to smooth muscle cell proliferation in normolipidemic wild-type mice, but it was unknown what would happen to hyperlipidemic apolipoprotein E-deficient (Apoe$^{-/-}$) mice. Examination of these mice revealed rapid development of atherosclerotic lesions in completely ligated carotid arteries within 4 weeks. Mice were fed a Western diet, starting 1 week before ligation, or a chow diet. Foam cell lesions formed as early as 1 week after ligation in mice fed the Western diet and 2 weeks in mice fed the chow diet. Fibrous lesions comprised of foam cells and smooth muscle cells and more advance lesions containing neovessels occurred at 2 and 4 weeks after ligation, respectively, in the Western diet group. Lesions were larger and more advanced in the Western diet group than the chow group. Neutrophil infiltration was observed in growing intimal lesions in both diet groups, while CD8+ T cells were found in lesions of chow-fed mice. This study demonstrates that Apoe$^{-/-}$ mice develop the entire spectrum of atherosclerosis in ligated carotid arteries in an accelerated manner and this model could be a valuable tool for investigating the development and therapy of atherosclerosis.

INTRODUCTION

Atherosclerosis is the primary cause of heart attack, ischemic stroke and peripheral arterial disease that kill more people than a single other disease in the Western countries [1]. Atherosclerotic lesions may directly or indirectly, through formation of thrombi, block the blood flow to such important organs as the heart and brain [2]. Angioplasty/stenting is a common and effective treatment to occlusive arterial diseases. However, a fraction of patients receiving the treatment develop significant restenosis, the reduction of the luminal size due to loss of gain in luminal size after angioplasty [2]. The placement of new-generation drug-eluting stents has dramatically reduced the incidence of post-interventional restenosis, down to ~10% within a 5-year period [3]. Most stent failures are attributable to in-stent thrombosis, neointimal hyperplasia and/or recurrent atherosclerosis.

The mouse is widely used to elucidate the pathological basis of various human diseases due to the availability of numerous inbred strains, knockouts and transgenics [4]. Neointimal hyperplasia can be induced in the common carotid artery of FVB/NJ mice by ligating the vessel near its distal end [5]. Smooth muscle cells can be observed in the intima as early as 5 days after ligation, their replication rate reaches its peak at 2 weeks, and by

4 weeks, intimal lesion sizes stop growing. Subsequent studies, however, indicate that neointimal growth in the ligated common carotid artery is very limited in most wild-type mouse strains, including C57BL/6 (B6) and C3H/HeJ [6]. In contrast, when deficient in apolipoprotein E (Apoe$^{-/-}$) and fed a high-fat diet, B6 mice developed prominent atherosclerotic lesions containing cholesterol clefts and intraplaque neovessels in partially ligated common carotid artery within 4 weeks [7]. However, no study has been carried out on Apoe$^{-/-}$ mice under either a chow or high fat diet condition to investigate lesion formation in a completely ligated carotid artery. These mice develop spontaneous hyperlipidemia and atherosclerosis on a low-fat, low cholesterol chow diet [8][9], which is accelerated by feeding a high-fat diet [10]. The primary aim of this study was to characterize lesion formation following complete ligation of one common carotid artery in Apoe$^{-/-}$ mice, including the types of cells present and the sequence of cellular events that occurred.

RESULTS

Plasma lipid levels of Apoe$^{-/-}$ mice

Plasma lipid levels were analyzed for Apoe$^{-/-}$ mice fed with a chow diet and a Western diet (Figure 1). As expected, these mice developed mild hyperlipidemia with a total cholesterol level of 308 ± 60 mg/dl on the chow diet and severe hyperlipidemia with a total cholesterol level of 858 ± 88 mg/dl on the Western diet. The HDL cholesterol levels were low on either diet (8 ± 2 mg/dl). Triglyceride levels were comparable between the chow and Western diet groups (159 ± 37 vs. 149 ± 19 mg/dl).

Lesion development

A complete ligation of the left common carotid artery of Apoe$^{-/-}$ mice caused no mortality within the 4-week observation period. Lesion formation in the ligated artery was evaluated at multiple time points under both chow and Western diet conditions. Intimal lesions appeared at 1 week after ligation on the Western diet and 2 weeks after ligation on the chow diet (Figure 2). With an increasing post-ligation duration, lesion sizes enlarged in both chow and Western diet groups. At 4 weeks after ligation, the average intimal lesion area of ligated carotid arteries was approximately 4-fold larger in the Western diet group than that in the chow diet group (112,987 ± 11,395 vs. 29,539 ± 7,001 μm^2/section; n=5 and 8, respectively). The difference was highly statistically significant (P = 0.00047).

The medial area of ligated carotid arteries was generally larger than the area of contralateral right carotid arteries at 1, 2 and 4 weeks after ligation, regardless of diet (Figure 2). At 4 weeks, the medial area of ligated carotid arteries had doubled the area of contralateral arteries in both diet groups. The areas within the external or internal elastic lamina in the ligated carotid arteries were comparable between the two diet groups at 1 and 2 weeks after ligation. However, at 4 weeks, these areas were approximately twice larger in the Western diet group than the chow diet group (P = 0.00077 and 0.001, respectively).

Histologically, intimal lesions at 1 week after ligation on the Western diet and 2 weeks on the chow diet possessed the nature of fatty streaks comprised primarily of foam cells (Figure 3B, 3D and 3E). These cells were larger than other cells in the lesions with a lightly stained cytoplasm and a foamy morphology on H&E sections. At 2 weeks after ligation on the Western diet, the intimal lesions were typical of fibrous plaques containing numerous foam cells covered by a fibrous cap (Figure 3E). At 4 weeks, intimal lesions of both diet groups progressed to more advanced stages, containing neovessels and substantially narrowing the arterial lumen (Figure 3C and 3F).

The intimal lesions of ligated arteries from either diet group intensely stained with oil red O, suggesting richness in lipids (Figure 4). The medial layer of ligated arteries showed little staining at 2 weeks after ligation (Figure 4A) but grossly stained at 4 weeks on sections from mice fed the chow diet (Figure 4B). The medial layer intensely stained with oil red O at both time points on sections from mice fed the Western diet (Figure 4D and 4E). The contralateral right common carotid artery developed no lesions in either diet group. The medial layer of the artery showed little staining (Figure 4C and 4F).

Cytological changes during intimal lesion formation

One day after ligation, neutrophils were found to be attached to the endothelium of carotid arteries (Figure 5A). Neutrophil infiltration was also observed in growing intimal lesions and at the interface with the medial layer (Figure 5B). This infiltration was observed in ligated arteries of both diet groups.

Immunoreactivity to vWF was not obvious in the ligated carotid artery at 1 day after ligation, but a dense stain was observed in regions of the intima or intimal lesions at day 3 and all subsequent time points in both diet groups (Figure 6). Four weeks after ligation, strong immunoreactivity to vWF was observed not only in intimal lesions but also throughout the medial wall of ligated arteries in the Western diet group.

No macrophages were detectable in the ligated carotid arteries of either diet group at earlier time points (Figure 7). Macrophage staining in intimal lesions was obvious at later time points, such as 2 and 4 weeks after ligation, especially in mice fed the Western diet.

Immunoreactivity to α-smooth muscle actin was observed in the medial layer of arterial walls and fibrous

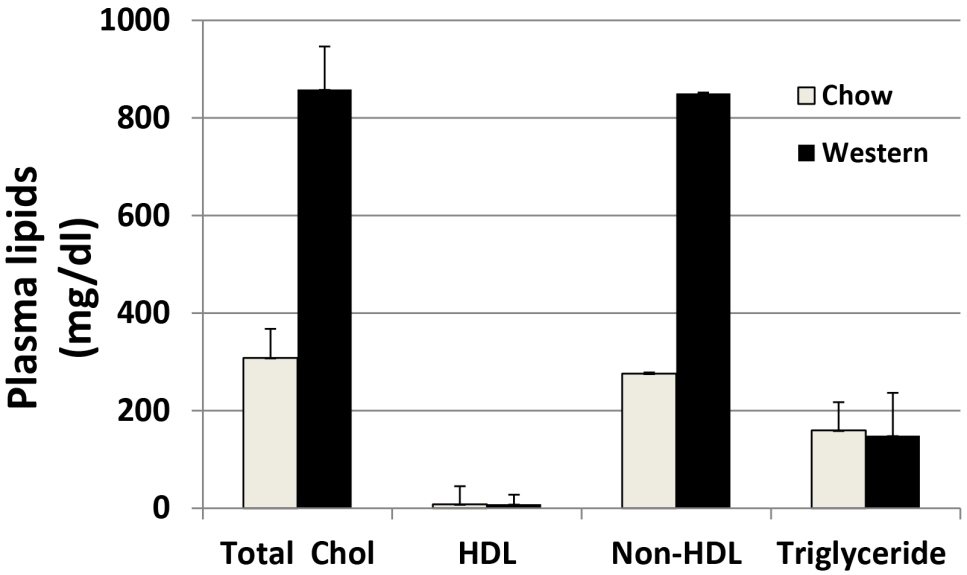

Figure 1: Plasma levels of total cholesterol (total chol), HDL cholesterol, and triglyceride in Apoe$^{-/-}$ mice fed a chow diet and a Western diet. Blood samples were obtained after mice were fasted overnight. Values are means ± SE for 3 or 5 male mice per group.

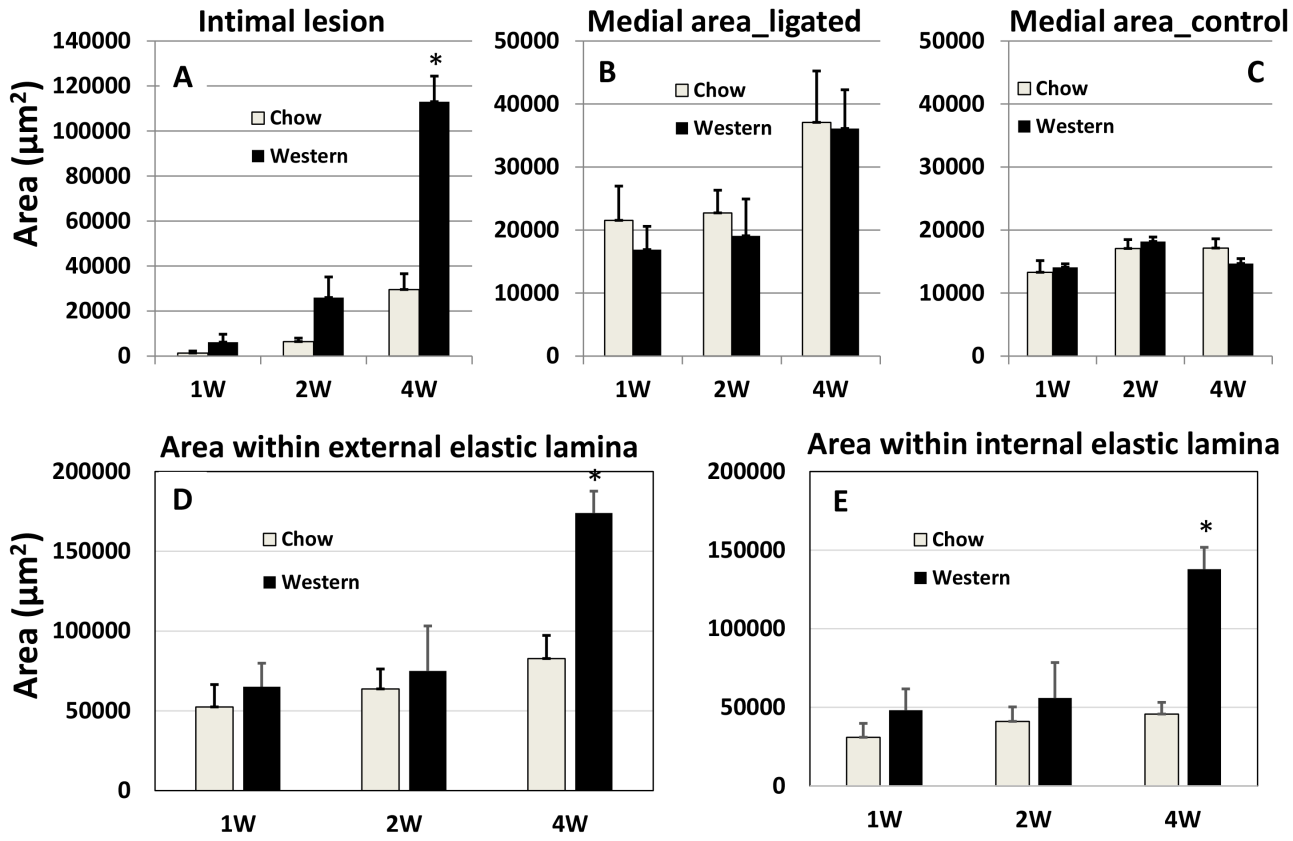

Figure 2: Quantitative measurements of intimal **(A)** and medial areas **(B)** in ligated left common carotid arteries and medial areas in the contralateral common carotid arteries **(C)** of Apoe$^{-/-}$ mice fed with a chow diet and a Western diet. Cross-sectional areas encircled by the external elastic lamina **(D)** and internal elastic lamina **(E)** in the ligated arteries were also presented. Measurements were made on the carotid arteries 1, 2 and 4 weeks after ligation. Values are means ± SE of 3~8 mice per group. * $P < 0.05$ versus mice fed a chow diet.

caps covering intimal lesions (Figure 8). The medial layer at 4 weeks after ligation appeared visiblly disorganized and thickened in both diet groups.

T lymphocytes were identified with antibodies targeting CD4 and CD8 antigens. Immunoreactivity to the CD8 antigen was observed in intimal lesions and adjacent medial walls in the chow diet group (Figure 9). In contrast, CD8+ T cells were not detectable in the Western diet group. Immunostaining with an antibody directed against CD4 antigen revealed no signal, indicating the absence of CD4+ T cells in the lesions (data not shown).

DISCUSSION

Partial ligation leads to rapid development of atherosclerosis in the common carotid artery of Apoe$^{-/-}$ mice due to disturbed blood flow [7], but it was unknown what would happen if blood flow was completely blocked. In this study, we characterized intimal lesion formation in completely ligated common carotid arteries of Apoe$^{-/-}$ mice when fed both a chow diet and a Western diet. We found that Apoe$^{-/-}$ mice developed the entire spectrum of atherosclerotic lesions in the ligated artery in an accelerated fashion. Both male and female mice were included in this study as previous studies showed that sex made no difference in intimal lesion formation in ligated common carotid artery of either wild-type B6 mice [11] or Apoe$^{-/-}$ mice [7]. The intimal lesions formed in the ligated carotid artery of Apoe$^{-/-}$ mice bear the histological features of atherosclerotic lesions that develop spontaneously at such sites as arterial branches and curves. Foam cells, the hall mark of atherosclerotic lesions, were observed in the ligated vessels of Apoe$^{-/-}$ mice fed either diet. Both H&E staining and immunocytochemical analysis demonstrated the abundance of lipid-laden, macrophage-derived foam cells in the intimal lesions, especially in mice fed the Western diet. On H&E sections, foam cells are easily recognizeable due to their foamy morphology. Fibrous cap, cholesterol cleft, and neovessels of atherosclerotic plques are also identifiable. Our previous studies demonstrate the reliability of H&E staining in identification of lipid-laden foam cells and neovessels [12] [13][14]. Initially, the lesions contained no smooth muscle cells. As they progressed, smooth muscle cells appeared, most of which were located in fibrous caps covering the foam cell-rich areas. As the lesions continued to progress, neocapillaries appeared. Intraplaque neovascularization is considered a major feature of an advanced atherosclerotic lesion [15]. In this study, H&E staining clearly revealed the presence of intraplaque vascular structures. The strong immunoreactivity to the von Willebrand factor (vWF) in lesion areas also suggests the abundance of

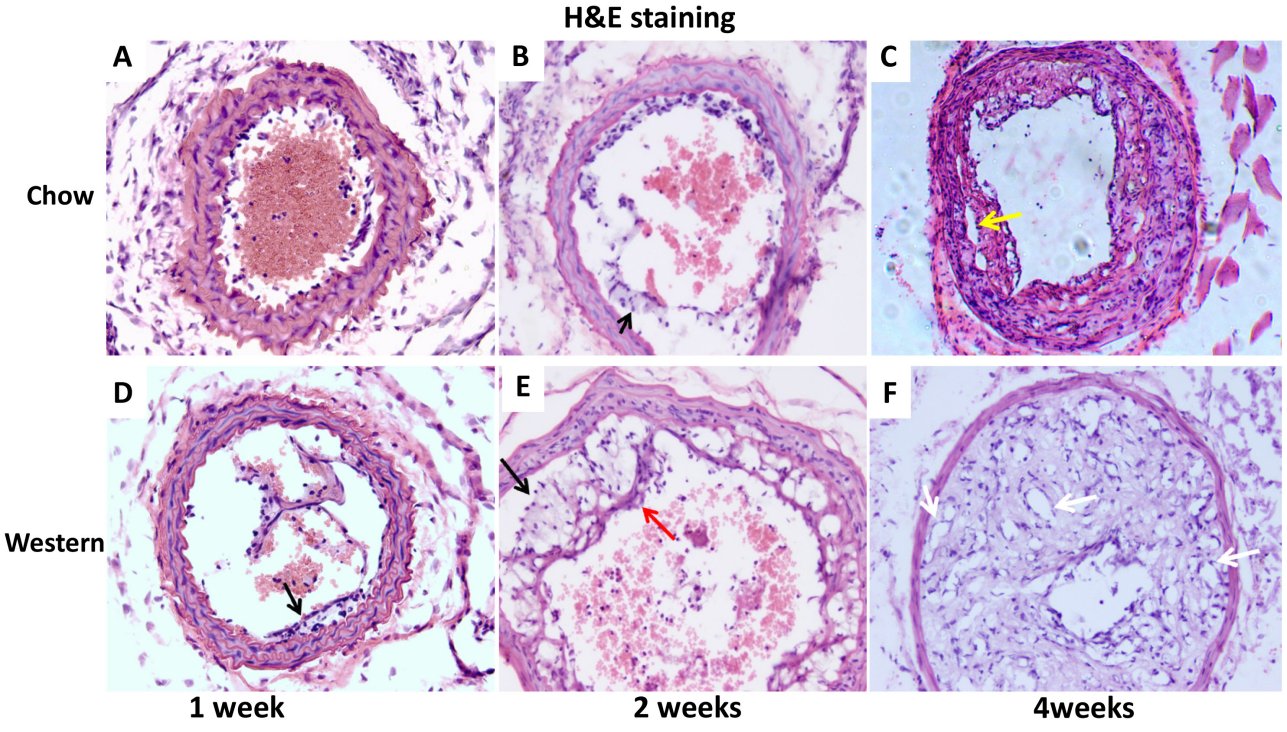

Figure 3: Representative photographs of cross-sections of ligated common carotid arteries from Apoe$^{-/-}$ mice 1, 2 and 4 weeks after ligation. The top row shows cross sections of the vessels from mice fed a chow diet **(A, B, C)**, and the bottom row shows cross sections from mice fed a Western diet **(D, E, F)**. Black arrows point at foam cells, red arrow at fibrous cap, white arrows at neovessels, and yellow arrow at cholesterol cleft. Sections were stained with the standard hematoxylin-eosin (H&E) method. Original magnification: ×20.

endothelial cells in the plaques. It is noteworthy that neovascularization was also found in the medial arterial wall underlying the advanced lesions, which probably contributed to the disorientation of smoth muscle cells and the strong immunoreactivity to vWF in the medial layer (Figures 6 and 8). In the advanced stage, the lesions continued to increase in size and increasingly occluded the lumen of ligated arteries.

A previous study reported that partial ligation of the common carotid artery resulted in rapidly developed atherosclerotic lesions in Apoe$^{-/-}$ mice fed a high fat diet [7]. The study has attributed the accelerated atherogenesis to disturbed blood flow. In the present study, we completely ligated the common carotid artery in its distal end and still observed rapidly progressed atherosclerosis in the vessel under a similar dietary condition. Complete ligation in the distal end near the bifurcation caused blood stasis and flow cessation in the common carotid artery although the vessel still experienced arterial blood pressure and pulsation. Thus, the current finding suggests that the shear stress from blood flow is not crucial to the development of atherosclerosis.

Intimal lesion formation in a ligated carotid artery is often limited in most wild-type mouse strains, including B6 mice [6]. In contrast, moderate to significantly sized intimal lesions are observed in B6-Apoe$^{-/-}$ mice, especially when fed a Western diet. The absence of Apoe and the resultant hyperlipidemia should be responsible for enhanced lesion formation in B6-Apoe$^{-/-}$ mice. Indeed, Apoe has been shown to inhibit and hyperlipidemia to promote smooth muscle cell proliferation and vascular remodeling [16][13].

Intense staining for vWF in the intimal region of ligated arteries was observed as early as 3 days after ligation and during the latter observation period. The early vWF stain was probably resultant from increased endothelial secretion as well as the platelet deposition on the surface of the endothelium. Upon adhesion, platelets are activated and secrete pro-inflammatory cytokines and chemoattractants, which promote leukocyte binding to inflamed or atherosclerotic endothelium [17]. Platelets as well as platelet-covered leukocytes have been found to line the endothelium of ligated carotid artery within days [18]. The strong vWF stain was observed in the intimal lesions of mice fed the Western diet. This is in agreement

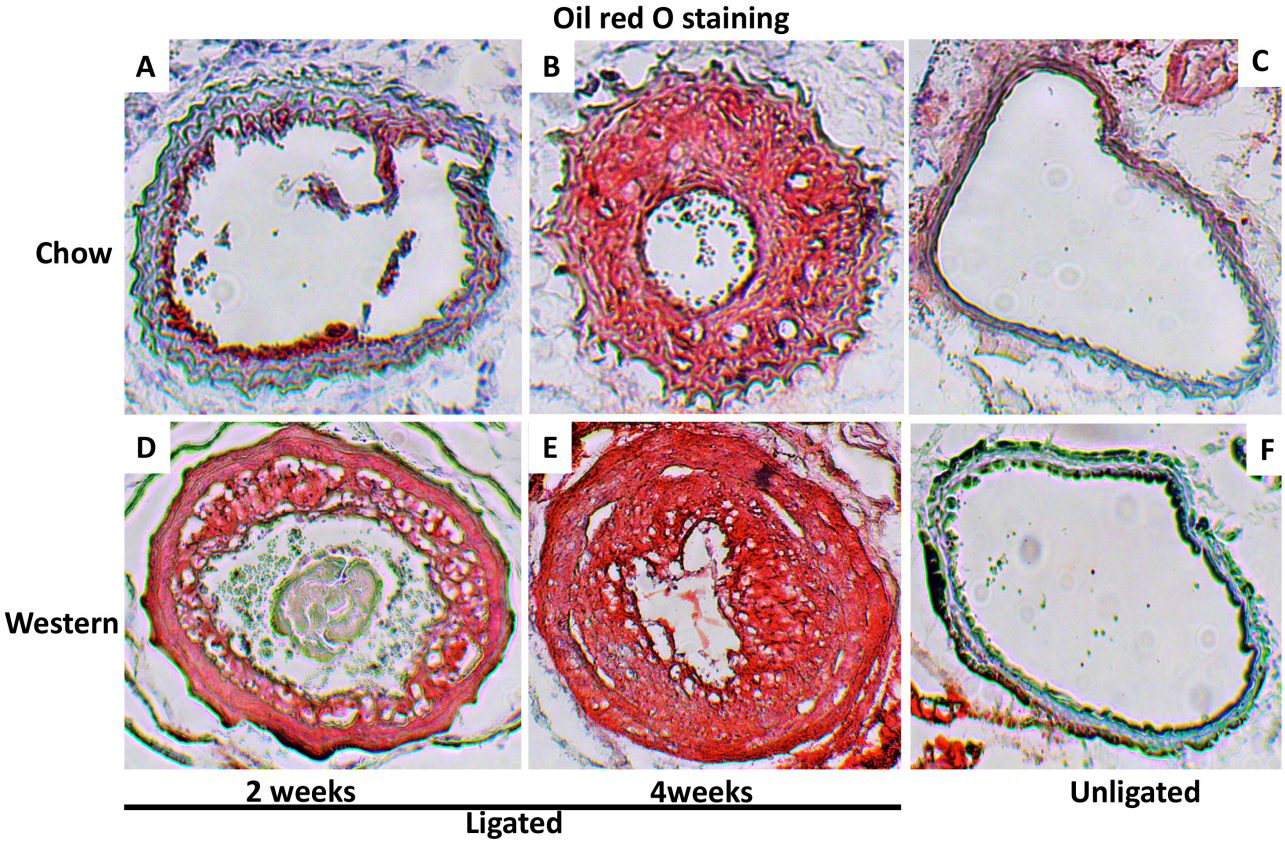

Figure 4: Cross-sections of ligated common carotid arteries **(A, B, D, E)** and unligated right carotid arteries **(C, F)** stained with oil red O. Note intense staining of intimal lesions in the ligated arteries of Apoe$^{-/-}$ mice fed either chow or Western diet and in the medial layer of ligated arteries in mice fed the Western diet. There were no lesions in the unligated carotid arteries. Original magnification: ×10.

with what was observed in rabbits where high-fat diet induces vWF production and enhances platelet adhesion to subendothelial plaque regions [19]. The enhanced vWF expression in the lesions could partially be attributable to the synthesis and secretion by intraplaque neovessels.

The present study showed an early interaction of neutrophils with endothelial cells in the ligated carotid artery. Neutrophil adherence to endothelial cells was observed one day after ligation, the earliest time point examined. Activated neutrophils release superoxide and pro-inflammatory molecules at the sites of adhesion that promote the recruitment of monocytes and alter endothelial cell properties [20]. A recent study shows that in hypercholesterolemia-induced neutrophilia, cholesterol crystals trigger neutrophils to release neutrophil extracellular traps, which prime macrophages for cytokine

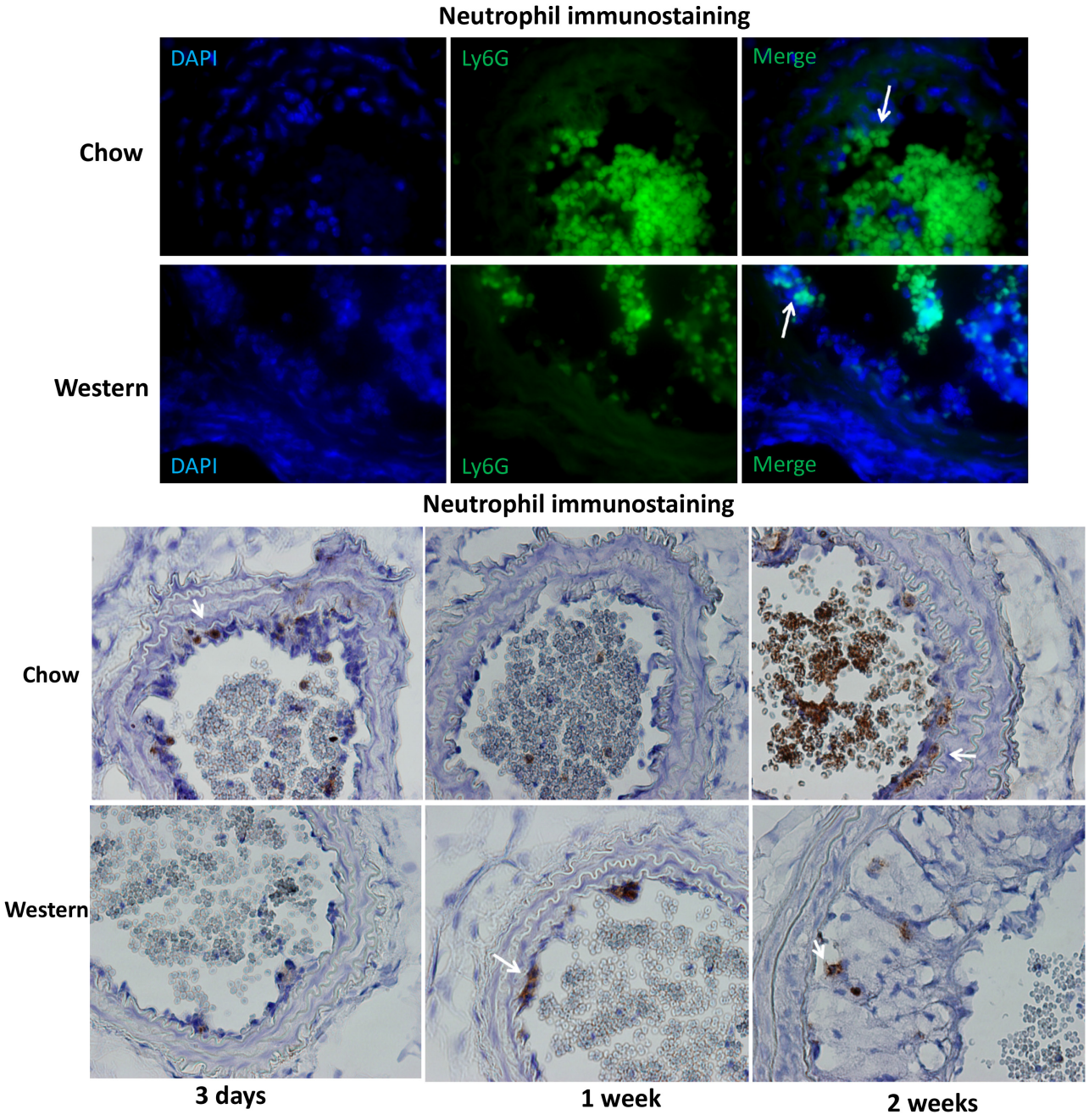

Figure 5: Immunocytochemical detection of neutrophils in the ligated carotid artery of Apoe-/- mice fed a chow or Western diet. (A) sections were stained with FITC conjugated anti-neutrophil antibody (green) and DAPI (blue). Arrows point to neutrophils attached to the endothelium. **(B)** section stained with the standard Avidin-Biotin Complex (ABC) method using a biotinated anti-neutrophil antibody. Arrows point to stained neutrophils.

release and activate T helper 17 cells and consequently amplify immune cell recruitment in atherosclerotic plaques [21].

An interesting finding of this study is that CD8+ T cells were only observed in the intimal lesions of mice fed the chow diet but not those fed the Western diet. The oxysterol metabolite, 27-hydroxycholesterol, from high fat diet suppresses the recruitment of CD8+ T lymphocytes to peripheral tissues [22]. We previously found that high fat diet induces a chronic inflammatory status with elevated production of proinflammary cytokines in mice [23][24] [13][25]. CD8+ T cells promote reendothelialization and inhibit neointima formation following arterial injury in mice [26]. Clinical studies indicate that the neutrophil to lymphocyte ratio reflects the severity of diseases with an inflammatory component and predicts the risk of developing in-stent restenosis and major adverse cardiac events [27][28]. Thus, there is a possibility that the Western diet promotes intimal lesion formation in the ligated carotid artery through action on CD8+ T cells.

On the Western diet, Apoe$^{-/-}$ mice showed a dramatic increase in total cholesterol levels, primarily

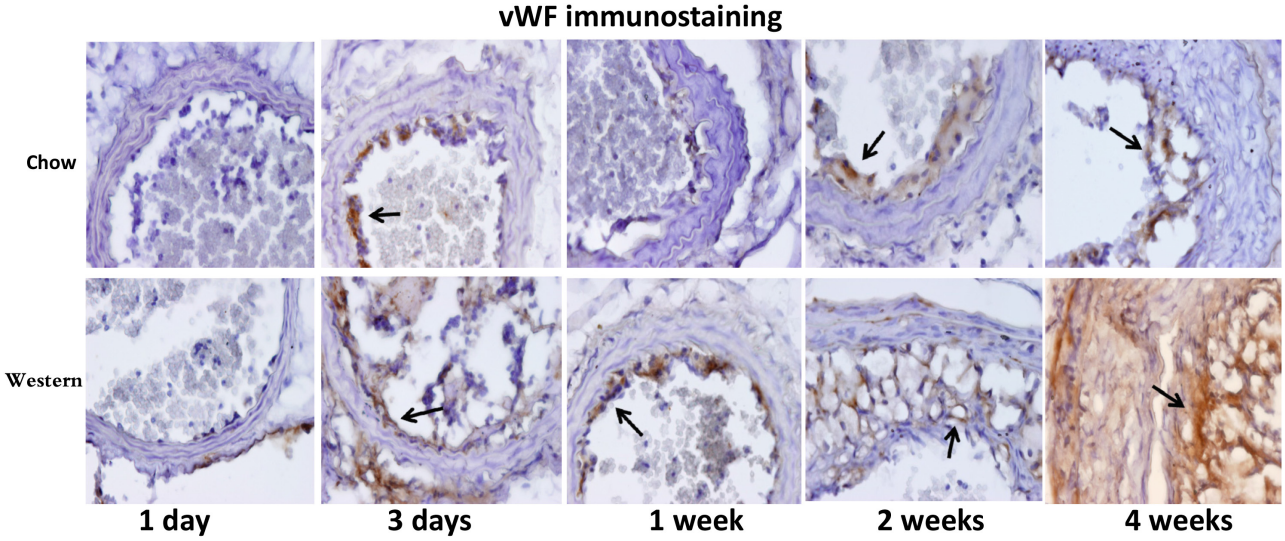

Figure 6: Immunohistochemical staining for von Willebrand Factor (VWF) in the ligated carotid arteries of Apoe$^{-/-}$ mice fed a chow diet (top row) or a Western diet (bottom row) 1 day, 3 days, 1, 2 and 4 weeks after ligation. Arrows point to stained areas.

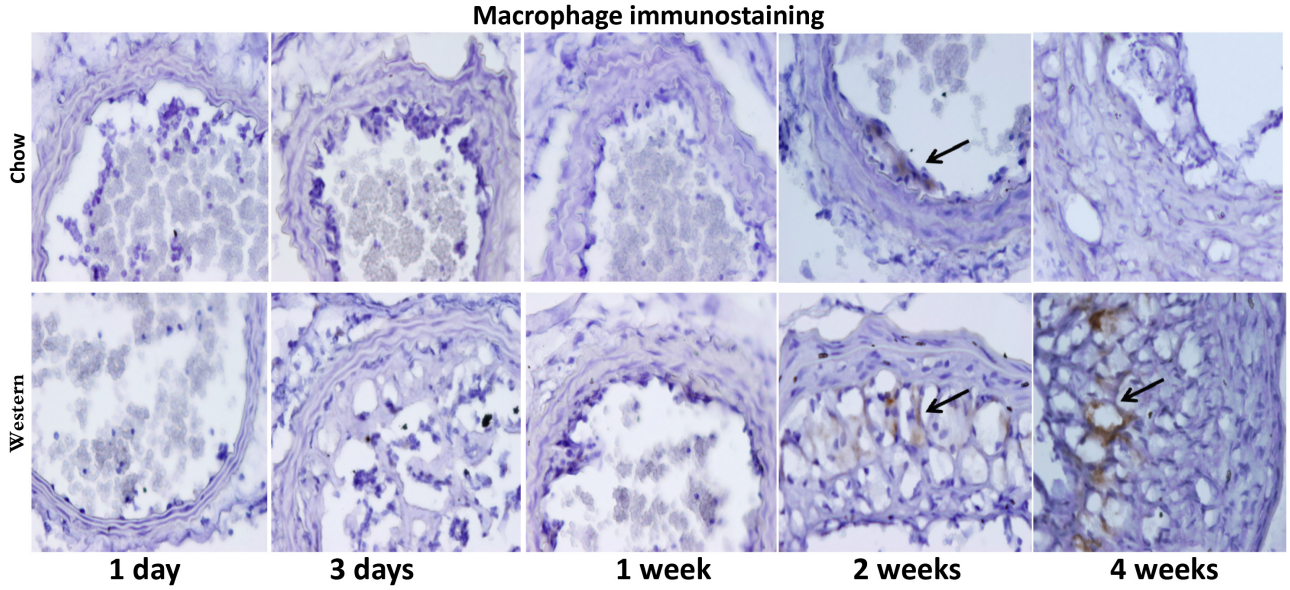

Figure 7: Immunocytochemical detection of macrophages in ligated carotid arteries of Apoe$^{-/-}$ mice with different post-ligation durations. The top row shows sections from mice fed a chow diet, and the bottom row shows sections from mice fed a Western diet. Arrows point to stained areas.

due to elevations in non-HDL cholesterol, and exhibited accelerated atherosclerotic lesion formation. The lesions in Apoe$^{-/-}$ mice fed the Western diet occurred earlier and were more advanced compared to those in chow fed mice. Besides the effect on cholesterol homeostasis, high fat diet induces a chronic inflammatory status with elevations in circulating proinflammatory molecules, such as VCAM-1, P-selection and MCP-1 [24][25]. Thus, the Western diet accelerated the atherogenic process also through action on inflammation.

An intriguing finding in the present study is that the intimal lesions contained numerous neovessels, especially in mice fed the Western diet. Neoangiogenesis is a histological feature of advanced atherosclerosis in humans [29], but it is rarely seen in animal models, including Apoe$^{-/-}$ mice [30]. Hypoxia has been observed in atherosclerotic plaques [31][32] and considered a major factor behind neoangiogenesis. The rapid progression of intimal lesions and the static blood flow following carotid

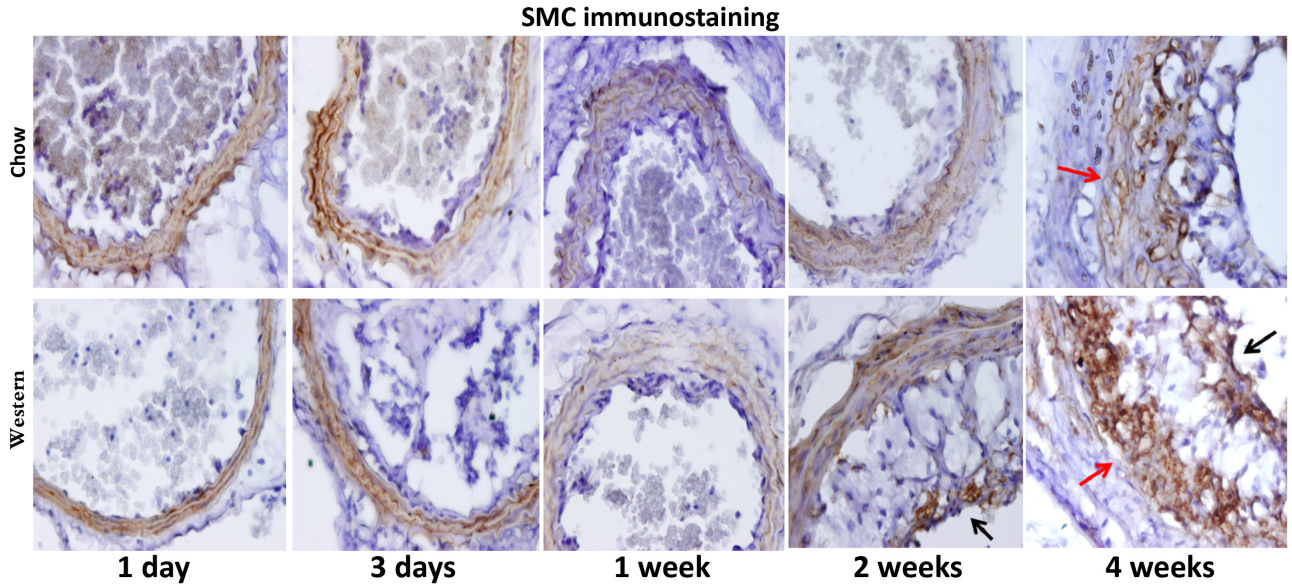

Figure 8: Immunohistochemical staining for α-smooth muscle actin in the ligated carotid artery of Apoe$^{-/-}$ mice fed a chow diet (top row) or a Western diet (bottom row) with different post-ligation durations. Note the disorganization of the medial layer 4 weeks after ligation (denoted by red arrow). Black arrows point to stained areas in the cap.

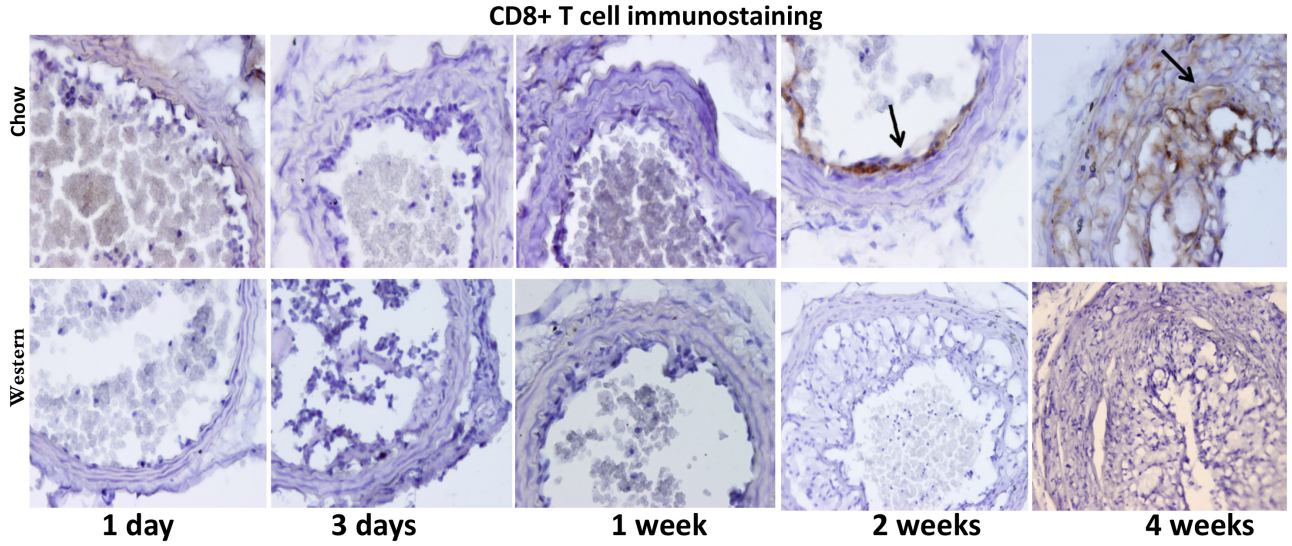

Figure 9: Immunohistochemical staining for CD8 T cells in ligated carotid arteries of Apoe$^{-/-}$ mice 1 day, 3 days, 1, 2 and 4 weeks after ligation. The top row shows staining in cross sections from mice fed a chow diet, and the bottom row shows staining in sections from mice fed a Western diet. Note the presence of CD8+ cells in intimal lesions of mice fed a chow diet (denoted by arrow) but not a Western diet.

ligation undoubtedly have aggravated hypoxia in the lesions and consequently accelerated neovessel formation.

In wild-type mouse strains, ligation of the carotid artery causes constriction or shrinkage of the vessel diameter [5][6]. In contrast, such alterations were not found in Apoe$^{-/-}$ mice fed either a chow or Western diet; rather these mice showed an increase in the areas within the internal and external elastic laminae 4 weeks after ligation. This finding is consistent with the vascular remodeling observed in animal models of atherosclerosis and in human coronary arteries with plaques [33][34][35]. Smooth muscle cells are the main component of intimal lesions in wild-type mice [5], while in Apoe$^{-/-}$ mice the intimal lesions contain numerous macrophages. Smooth muscle cells and the extracellular matrix produced by the cells restricts vessel distension [36]. In contrast, macrophages produce MMP-9, MMP-12, and other enzymes that degrade extracellular matrix [37]. The degradation of the extracellular matrix is not only toward to the luminal side of the plaque but also toward the abluminal layer, thus weakening the vessel wall [37]. Moreover, a higher macrophage count and lipid content has shown significant associations with positive remodeling in human coronary artery with plaques [38][39].

In summary, the present study demonstrates that complete carotid ligation results in accelerated atherosclerosis, which rapidly progresses from fatty streak to fibrous lesion to advanced lesion, in Apoe$^{-/-}$ mice. This forms a striking contrast with the slow growth of atherosclerotic lesions in unligated carotid artery of Apoe$^{-/-}$ mice [40]. This model should be a valuable tool for studying the pathogenesis and therapeutic interventions of atherosclerosis.

MATERIALS AND METHODS

Mice

B6-Apoe$^{-/-}$ mice purchased from the Jackson Laboratory were bred to generate mice used for the present study. Mice of both sexes were weaned at 3 weeks of age onto a standard chow diet. One group of mice were maintained on a rodent chow diet throughout the entire experimental period. And the other group was fed a Western diet containing 21% fat, 48.5% carbohydrate, 17% protein, and 0.2% cholesterol (by weight) (TD 88137, Envigo), starting 1 week before surgery and being maintained on the diet thereafter. All procedures were carried out under the current NIH guidelines and approved by the Institutional Animal Care and Use Committee.

Surgical procedure

Ligation of the left common carotid artery was performed as previously described [14]. Briefly, mice aged 4~8 weeks were anesthetized by intramuscular injection with ketamine (80 mg/kg body weight; Ketaset, Aveco Inc.) and xylazine (8 mg/kg; AnaSed, Lloyd Laboratories). The left common carotid artery was dissected under a microscope and ligated near its bifurcation to completely block blood flow. The skin incision was then closed with a surgical glue (VETCLOSETM, Henry Schein Animal Health). Animals were euthanized 1 day, 3 days, and 1, 2, and 4 weeks after surgery. 3 or more mice were analyzed at each time point for each diet group.

Tissue preparation and lesion quantification

Mice were euthanized with prolonged exposure to isofluorane inhalation. The vasculature was perfused with 4% paraformaldehyde via the left ventricle of the heart. The neck was dissected and further fixed in the same solution for >24 h. After fixation, the front soft tissues of the neck encompassing the left and right common carotid were dissected out, embedded in OCT compound (Tissue-Tek, Miles Inc), and cross-sectioned in 10-μm thickness. Serial sections were collected, starting from disappearance of the ligation suture, and mounted on poly-D-lysine-coated slides with 6~8 sections per slide. Approximately 400 sections were collected for each mouse. Three evenly spaced slides were chosen for hematoxylin and eosin (H&E) staining. One section on each stained slide was subject to morphometric measurents of the ligated left common carotid artery and the contralateral right common carotid artery using Zeiss AxioVision 4.8 software. Luminal area and areas encircled by the internal and external elastic laminae were measured. Lesion area was calculated by subtracting the luminal area from the area surrounded by the internal elastic lamina, and the medial area of the arterial wall was calculated as the difference between the areas encircled by the external and internal elastic laminae. Measurements made from 3 separate slides were averaged for each vessel and this average was used for statistical analysis. For visualization of neutral lipid, selected sections were stained with oil red O and hematoxylin, counterstained with fast green [24].

Immunohistochemical analysis

Immunohischemical staining for smooth muscle cell α-actin, von Willebrand factor (vWF), and leukocyte specific markers was performed on frozen sections of the carotid arteries using the following primary antibodies: Mouse anti-human α-smooth muscle actin IgG (Dako Corp.); rat anti-mouse macrophage/monocyte IgG, clone MOMA-2 (Serotec); rabbit anti-human von Willebrand factor (vWF) (Sigma); rat anti-mouse CD4 antibody (Millipore); rabbit anti-mouse CD8 IgG (Cell Signaling); rat anti-mouse Ly-6G antibody (eBioscience); and FITC anti-mouse Ly-6G IgG (BD Biosciences). Subsequent incubations with biotinylated secondary

antibody and VECTASTAIN Elite ABC HRP Kit (Vector Laboratories) were performed as previously described [41]. Sections stained with fluorescent-labeled antibody or DAPI fluoromount-G (Southern Biotech) were directly visualized with a fluorescence microscope.

Plasma lipid measurements

Mice were fasted overnight before blood was collected through retro-orbital sinus puncture under isoflurane anesthesia. Plasma total cholesterol, HDL cholesterol, and triglyceride levels were measured using the Thermo DMA (Louisville, CO) cholesterol and triglyceride kits [16]. Non-HDL was calculated as the difference between total and HDL cholesterol levels.

Statistical analysis

All values were expressed as mean ± SE, with "n" indicating the number of mice. Student's t test was used to determine statistical differences between the two groups for morphometric measurements and plasma parameters. Differences were considered statistically significant at $P \leq 0.05$.

Author contributions

ZC, CH, ATG, WS designed and conduct the study, analyzed the data and draft the manuscript. JZ and QG supervised the study by ZC and CH. All authors read and approved the final manuscript.

CONFLICTS OF INTEREST

Authors declared no conflict of interest, including financial or personal relationships, which could have inappropriately influenced the work reported in this article.

GRANT SUPPORT

This work was supported by National Institutes of Health grants DK097120 and HL112281.

Chaoji Huangfu is the recipient of a scholarship from the Ministry of Higher Education of China.

Andrew Grainger is a recipient of the Robert R. Wagner Fellowship from the University of Virginia School of Medicine.

Data and materials availability

All raw data used in this study are available under Supplementary Materials.

REFERENCES

1. Mozaffarian D, Benjamin EJ, Go AS, Arnett DK, Blaha MJ, Cushman M, Das SR, de Ferranti S, Despres JP, Fullerton HJ, Howard VJ, Huffman MD, Isasi CR, et al, and Writing Group Members. Executive summary: heart disease and stroke statistics--2016 update: a report from the American Heart Association. Circulation. 2016; 133:447-454.
2. Fattori R, Piva T. Drug-eluting stents in vascular intervention. Lancet. 2003; 361:247-249.
3. Byrne RA, Joner M, Kastrati A. Stent thrombosis and restenosis: what have we learned and where are we going? The Andreas Gruntzig Lecture ESC 2014. Eur Heart J. 2015; 36:3320-3331.
4. Bharadwaj D, Mold C, Markham E, Du Clos TW. Serum amyloid P component binds to Fc gamma receptors and opsonizes particles for phagocytosis. J Immunol. 2001; 166:6735-6741.
5. Kumar A, Lindner V. Remodeling with neointima formation in the mouse carotid artery after cessation of blood flow. Arterioscler Thromb Vasc Biol. 1997; 17:2238-2244.
6. Harmon KJ, Couper LL, Lindner V. Strain-dependent vascular remodeling phenotypes in inbred mice. Am J Pathol. 2000; 156:1741-1748.
7. Nam D, Ni CW, Rezvan A, Suo J, Budzyn K, Llanos A, Harrison D, Giddens D, Jo H. Partial carotid ligation is a model of acutely induced disturbed flow, leading to rapid endothelial dysfunction and atherosclerosis. Am J Physiol Heart Circ Physiol. 2009; 297:H1535-543.
8. Plump AS, Smith JD, Hayek T, Aalto-Setala K, Walsh A, Verstuyft JG, Rubin EM, Breslow JL. Severe hypercholesterolemia and atherosclerosis in apolipoprotein E-deficient mice created by homologous recombination in ES cells. Cell. 1992; 71:343-353.
9. Zhang SH, Reddick RL, Piedrahita JA, Maeda N. Spontaneous hypercholesterolemia and arterial lesions in mice lacking apolipoprotein E. Science. 1992; 258:468-471.
10. Liu S, Li J, Chen MH, Liu Z, Shi W. Variation in type 2 diabetes-related phenotypes among apolipoprotein E-deficient mouse strains. PLoS One. 2015; 10:e0120935.
11. Korshunov VA, Berk BC. Flow-induced vascular remodeling in the mouse: a model for carotid intima-media thickening. Arterioscler Thromb Vasc Biol. 2003; 23:2185-2191.
12. Shi W, Pei H, Fischer JJ, James JC, Angle JF, Matsumoto AH, Helm GA, Sarembock IJ. Neointimal formation in two apolipoprotein E-deficient mouse strains with different atherosclerosis susceptibility. J Lipid Res. 2004; 45:2008-2014.
13. Tian J, Pei H, Sanders JM, Angle JF, Sarembock IJ, Matsumoto AH, Helm GA, Shi W. Hyperlipidemia is a major determinant of neointimal formation in LDL receptor-deficient mice. Biochem Biophys Res Commun. 2006; 345:1004-1009.
14. Shi W, Hu F, Kassouf W, Michel RP. Altered reactivity of pulmonary vessels in postobstructive pulmonary vasculopathy. J Appl Physiol (1985). 2000; 88:17-25.
15. Doyle B, Caplice N. Plaque neovascularization and antiangiogenic therapy for atherosclerosis. J Am Coll Cardiol. 2007; 49:2073-2080.

16. Zhu B, Kuhel DG, Witte DP, Hui DY. Apolipoprotein E inhibits neointimal hyperplasia after arterial injury in mice. Am J Pathol. 2000; 157:1839-1848.
17. Davi G, Patrono C. Platelet activation and atherothrombosis. N Engl J Med. 2007; 357:2482-2494.
18. Kawasaki T, Dewerchin M, Lijnen HR, Vreys I, Vermylen J, Hoylaerts MF. Mouse carotid artery ligation induces platelet-leukocyte-dependent luminal fibrin, required for neointima development. Circ Res. 2001; 88:159-166.
19. De Meyer GR, Hoylaerts MF, Kockx MM, Yamamoto H, Herman AG, Bult H. Intimal deposition of functional von Willebrand factor in atherogenesis. Arterioscler Thromb Vasc Biol. 1999; 19:2524-2534.
20. Soehnlein O, Weber C, Lindbom L. Neutrophil granule proteins tune monocytic cell function. Trends Immunol. 2009; 30:538-546.
21. Warnatsch A, Ioannou M, Wang Q, Papayannopoulos V. Inflammation. Neutrophil extracellular traps license macrophages for cytokine production in atherosclerosis. Science. 2015; 349:316-320.
22. Baek AE, Yu YA, He S, Wardell SE, Chang CY, Kwon S, Pillai RV, McDowell HB, Thompson JW, Dubois LG, Sullivan PM, Kemper JK, Gunn MD, et al. The cholesterol metabolite 27 hydroxycholesterol facilitates breast cancer metastasis through its actions on immune cells. Nat Commun. 2017; 8:864.
23. Li J, Wang Q, Chai W, Chen MH, Liu Z, Shi W. Hyperglycemia in apolipoprotein E-deficient mouse strains with different atherosclerosis susceptibility. Cardiovasc Diabetol. 2011; 10:117.
24. Tian J, Pei H, James JC, Li Y, Matsumoto AH, Helm GA, Shi W. Circulating adhesion molecules in apoE-deficient mouse strains with different atherosclerosis susceptibility. Biochem Biophys Res Commun. 2005; 329:1102-1107.
25. Yuan Z, Su Z, Miyoshi T, Rowlan JS, Shi W. Quantitative trait locus analysis of circulating adhesion molecules in hyperlipidemic apolipoprotein E-deficient mice. Mol Genet Genomics. 2008; 280:375-383.
26. Zhang JM, Wang Y, Miao YJ, Zhang Y, Wu YN, Jia LX, Qi YF, Du J. Knockout of CD8 delays reendothelialization and accelerates neointima formation in injured arteries of mouse via TNF-alpha inhibiting the endothelial cells migration. PLoS One. 2013; 8:e62001.
27. Balta S, Ozturk C, Balta I, Demirkol S, Demir M, Celik T, Iyisoy A. The neutrophil-lymphocyte ratio and inflammation. Angiology. 2016; 67:298-299.
28. Li C, Zhang F, Shen Y, Xu R, Chen Z, Dai Y, Lu H, Chang S, Qian J, Wang X, Ge J. Impact of neutrophil to lymphocyte ratio (NLR) index and its periprocedural change (NLRDelta) for percutaneous coronary intervention in patients with chronic total occlusion. Angiology. 2016.
29. Stefanadis C, Antoniou CK, Tsiachris D, Pietri P. Coronary atherosclerotic vulnerable plaque: current perspectives. J Am Heart Assoc. 2017.
30. de Vries MR, Quax PH. Plaque angiogenesis and its relation to inflammation and atherosclerotic plaque destabilization. Curr Opin Lipidol. 2016; 27:499-506.
31. Sluimer JC, Gasc JM, van Wanroij JL, Kisters N, Groeneweg M, Sollewijn Gelpke MD, Cleutjens JP, van den Akker LH, Corvol P, Wouters BG, Daemen MJ, Bijnens AP. Hypoxia, hypoxia-inducible transcription factor, and macrophages in human atherosclerotic plaques are correlated with intraplaque angiogenesis. J Am Coll Cardiol. 2008; 51:1258-1265.
32. Nie X, Laforest R, Elvington A, Randolph GJ, Zheng J, Voller T, Abendschein DR, Lapi SE, Woodard PK. PET/MRI of hypoxic atherosclerosis using 64Cu-ATSM in a rabbit model. J Nucl Med. 2016; 57:2006-2011.
33. Armstrong ML, Heistad DD, Marcus ML, Megan MB, Piegors DJ. Structural and hemodynamic response of peripheral arteries of macaque monkeys to atherogenic diet. Arteriosclerosis. 1985; 5:336-346.
34. Glagov S, Weisenberg E, Zarins CK, Stankunavicius R, Kolettis GJ. Compensatory enlargement of human atherosclerotic coronary arteries. N Engl J Med. 1987; 316:1371-1375.
35. Bonthu S, Heistad DD, Chappell DA, Lamping KG, Faraci FM. Atherosclerosis, vascular remodeling, and impairment of endothelium-dependent relaxation in genetically altered hyperlipidemic mice. Arterioscler Thromb Vasc Biol. 1997; 17:2333-2340.
36. Wagenseil JE, Mecham RP. Vascular extracellular matrix and arterial mechanics. Physiol Rev. 2009; 89:957-989.
37. Shi W, Brown MD, Wang X, Wong J, Kallmes DF, Matsumoto AH, Helm GA, Drake TA, Lusis AJ. Genetic backgrounds but not sizes of atherosclerotic lesions determine medial destruction in the aortic root of apolipoprotein E-deficient mice. Arterioscler Thromb Vasc Biol. 2003; 23:1901-1906.
38. Varnava AM, Mills PG, Davies MJ. Relationship between coronary artery remodeling and plaque vulnerability. Circulation. 2002; 105:939-943.
39. Ota H, Magalhaes MA, Torguson R, Negi S, Kollmer MR, Spad MA, Gai J, Satler LF, Suddath WO, Pichard AD, Waksman R. The influence of lipid-containing plaque composition assessed by near-infrared spectroscopy on coronary lesion remodelling. Eur Heart J Cardiovasc Imaging. 2016; 17:821-831.
40. Rosenfeld ME, Polinsky P, Virmani R, Kauser K, Rubanyi G, Schwartz SM. Advanced atherosclerotic lesions in the innominate artery of the ApoE knockout mouse. Arterioscler Thromb Vasc Biol. 2000; 20:2587-2592.
41. Yuan Z, Pei H, Roberts DJ, Zhang Z, Rowlan JS, Matsumoto AH, Shi W. Quantitative trait locus analysis of neointimal formation in an intercross between C57BL/6 and C3H/HeJ apolipoprotein E-deficient mice. Circ Cardiovasc Genet. 2009; 2:220-228.